Supporting Information for: Human Serotonin Receptor 5-HT1A Preferentially Segregates to the Liquid Disordered Phase in Synthetic Lipid Bilayers

M. Gertrude Gutierrez and Noah Malmstadt*

Mork Family Department of Chemical Engineering and Materials Science, University of Southern California, 925 Bloom Walk, Los Angeles, California 90089, United States

Email: malmstadt@usc.edu

Materials

1-palmitoyl-2-oleoyl-*sn*-glycero-3-phosphocholine (POPC), porcine brain sphingomyelin, (BSM), cholesterol (Chol), 1,2-dioleoyl-*sn*-glycero-3-phosphocholine (DOPC), 1,2-dipalmitoyl-*sn*-glycero-3-phosphocholine (DPPC) and biotin-1,2-dipalmitoyl-*sn*-glycero-3-phosphoethanolamine (DPPE) were acquired from Avanti Polar Lipids (USA) and used without further purification. ATTO-488-labeled DPPE was used as a fluorescent tag without further purification (ATTO-TEC, Germany). All reagents such as but not limited to agarose (Type IX, gel point 8-17˚C), phosphate buffered saline (PBS), sodium hydroxide (NaOH), sucrose, and glucose were of analytical grade (Sigma Aldrich, USA). Membrane fragments containing 5-HT_{1A} (Perkin Elmer, USA), 5-HT_{1A} antibodies (Thermo Fisher, USA), and 5HT1A-633-AN2, a fluorescent derivative of the well-known 5-HT_{1A} antagonist NAN-190 (Sigma Aldrich, USA), were used without further purification. Sykes-Moore chambers (Bellco, USA) and standard 25mm no. 1 glass coverslips (ChemGlass, USA) were used throughout. 18.2 MΩ cm Milli-Q water was used in all experiments (EMD Millipore, USA). Protein desalting micro spin columns (Thermo Scientific, USA) and NHS-rhodamine (Thermo Scientific, USA) were used as per the manufacturers' instructions.

Fabrication of vesicles and protein incorporation

25 mm no. 1 coverslips were cleaned via sonication in concentrated NaOH for 30 minutes at 35°C. Subsequent washing with water was performed to remove excess NaOH. Coverslips were further plasma treated in a PDC-32G benchtop plasma cleaner (Harrick Plasma, USA) for 15 minutes. Coverslips were held in Sykes-Moore chambers for vesicle formation.

Protein-incorporated GUVs were formed using the agarose hydration method as reported by Hansen *et al*, 2013[1] and adapted from methods reported by Horger *et al*, 2009.[2] Briefly, a 1:19 w/v mixture of membrane fragment suspension and agarose (2% w/v) was drop cast onto coverslips and a thin film was made. For control GUV fabrication, protein was omitted from the thin film and only 2% w/v agarose was used. The film was allowed to air dry at room temperature. Lipid solutions of 5 mg/ml in $CHCl_3$ containing 0.2% mol biotin-DPPE and 0.4% mol ATTO-488-DPPE were added drop wise to the protein-agarose film. Solvent was evaporated using a stream of N_2 gas. Lipids were rehydrated

with 200 mM sucrose in PBS (pH 7.4) above the gel-liquid transition temperature of all of the lipids (~45°C) for 20 minutes (See Figure S1 for an example of the swollen lipid film).

For individual imaging, GUVs were harvested from the coverslip and diluted in 3x 200 mM glucose in PBS (pH 7.4). GUVs were allowed to settle in glucose for 15 minutes at 45°C and then anchored to coverslips functionalized with BSA-biotin. Functionalized coverslips were freshly cleaned and treated with BSA-biotin (1% w/v) for 1 hour at room temperature, leading to physiosorption of BSA on the glass surface. Coverslips were then washed with Milli-Q water and exposed to avidin (1 mg/ml) immediately prior to anchoring individual GUVs. Antibody binding and antagonist binding was performed at 37°C and all imaging was performed at 30°C.[3,4]

Antibody labeling

5-HT_{1A} antibodies were equilibrated to room temperature and conjugated to NHS-rhodamine in DMSO at 10x molar excess. Sodium bicarbonate was added as per manufacturer's instructions to raise the pH to 8.0. The solution was allowed to react for one hour at room temperature. After one hour antibodies were desalted using spin columns according the manufacturer's instructions. Labeled antibody UV-vis absorbance was read on a NanoDrop ND-1000 (Thermo Fisher, USA). Antibody concentration was determined to be 7.7 mg/mL and labeling efficiency was calculated to be 0.83.

Antibody Binding Assay

GUVs previously prepared for individual imaging were exposed to 1:1000 rhodamine-labeled 5-HT_{1A} antibodies at 37°C for 1 hour. GUVs were imaged before and after to track the increased intensity at vesicle surfaces as a result of successful antibody binding (see Figure S2). Samples were subsequently washed with 200 mM glucose in PBS to remove excess fluorescent antibody. GUVs were imaged at 491 nm and 561 nm excitation corresponding to 523 nm and 575 nm emission respectively.

Antagonist Binding Assay

GUVs anchored to a glass coverslips of observation chambers were exposed to 1 mM of 5HT1A-633-AN2, a fluorescent derivative of the 5-HT_{1A} antagonist NAN-190. The concentration is 1-log unit above the K_d per product specification. Samples were incubated at 37°C for 10 minutes. GUVs were washed with 200 mM glucose in PBS to remove excess fluorophore and were imaged to observe antagonist binding at 491 nm and 640 nm excitation corresponding to 523 nm and 650 nm emission respectively.

Microscopy

Imaging was done on a TI-Eclipse inverted microscope (Nikon, Japan) equipped with a spinning-disc CSUX confocal head (Yokogawa, Japan) and a 16-bit Cascade II 512 EMCCD camera (Photometrics, USA). Excitation of fluorophores was done using 50 mW solid-state lasers at 491 nm, 561 nm, and 640 nm (Coherent Inc., Germany) at

200ms exposure time. All images were taken using a Plan-Apo 60x NA1.43 oil immersion Nikon objective. Z-stack images were separated by 0.5 μm steps. Temperature control during imaging was performed using a heating-cooling stage with a stability and accuracy of 0.1°C (Bioscience Tools, USA).

Image Processing

All images were processed and analyzed using ImageJ. Standard deviation projections of Z-stacks were produced using standard ImageJ stack tools. Fluorescent micrographs of GUVs using 491 nm excitation are shown using the ImageJ green lookup table, micrographs using 561 nm excitation are shown using the ImageJ red lookup table and all images using 640 nm excitation are shown using the ImageJ blue lookup table. All images are presented without any further processing adjustments or corrections and (with the exception of control images that show no objects) are scaled from minimum to maximum intensity. Images in which no objects could be discerned were adjusted to match intensity histogram of the rhodamine-band image in Figure 1C (Mean intensity: 1387.3, Standard Deviation: 3249.4, Minimum: 34.7, Maximum: 21711.7). The adjustment eliminated the artifactual apparent amplification of background noise that occurs if min-max scaling is applied to blank images. Images are presented as Z-stack projections unless otherwise specified. All other analysis was done using JMP.

Images of GUV yield from agarose hydration method

GUVs were labeled with 0.2 mol% ATTO-488-DPPE to facilitate fluorescent observation of vesicles. Upon rehydration of the lipid film on the agarose surface, vesicles could be seen to bud under the 491 nm excitation band (Figure S1). There was no detected signal at 561 nm excitation, indicating that the ATTO-488 dye had no significant bleed-through into the fluorescent bands that were used to image the antibody. GUVs were harvested from coverslips and settled in observation chambers. The size of typical vesicles yielded from agarose swelling ranges from 1μm to 50μm. A representative histogram for POPC systems can be found in Figure S1. This distribution is typical of all lipid system used in all studies described here.

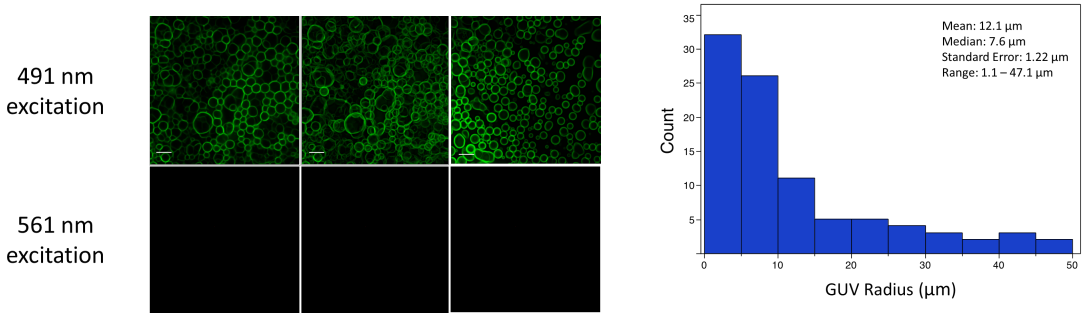

Figure S1. GUVs budding from protein-agarose thin film. Scale bars are 10 μm. Top images show fluorescence from 491 nm excitation showing ATTO-488 labeled lipid and bottom images show excitation at 561nm with no visible fluorescence. The histogram to

the right shows the typical vesicles size distribution for POPC lipid compositions (n=87). Mean GUV radius is 12.1 μm with a standard error of 1.22 μm and a range of 1.1 μm to 47.1 μm.

Antibody binding

Antibody binding could be observed prior to the induction of phase separation. GUVs were imaged prior to antibody exposure at both 491 nm and 561 nm excitation. After exposure to 1:1000 NHS-rhodamine conjugated 5-HT_{1A} polyclonal antibody for one hour at 37°C, GUVs were imaged and increased intensity at the edges (exterior) of vesicles was observed at 561 nm excitation. See Figure S2 and S3.

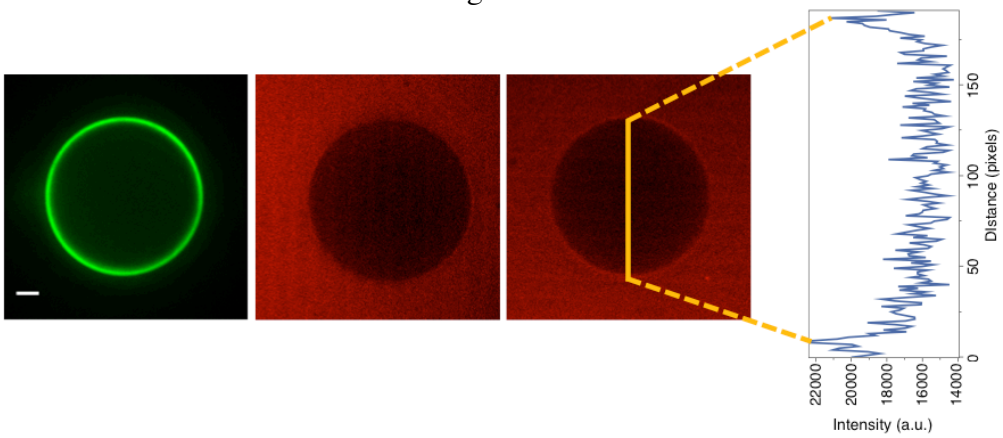

Figure S2. GUV intensity increase during antibody binding. Left micrograph shows GUV at 491 nm immediately after exposure to antibody. Middle micrograph shows GUV at 561 nm immediately after exposure to antibody. After one hour of incubation and prior to washing with 200mM glucose in PBS (pH 7.4) increased intensity is observed at the surface of the GUV (right micrograph). Scale bar is 5µm, all images are confocal slices. The plot show intensity of GUV at 561 nm excitation. Maximum intensity peaks correspond to the exterior of the vesicle and indicate successful antibody binding.

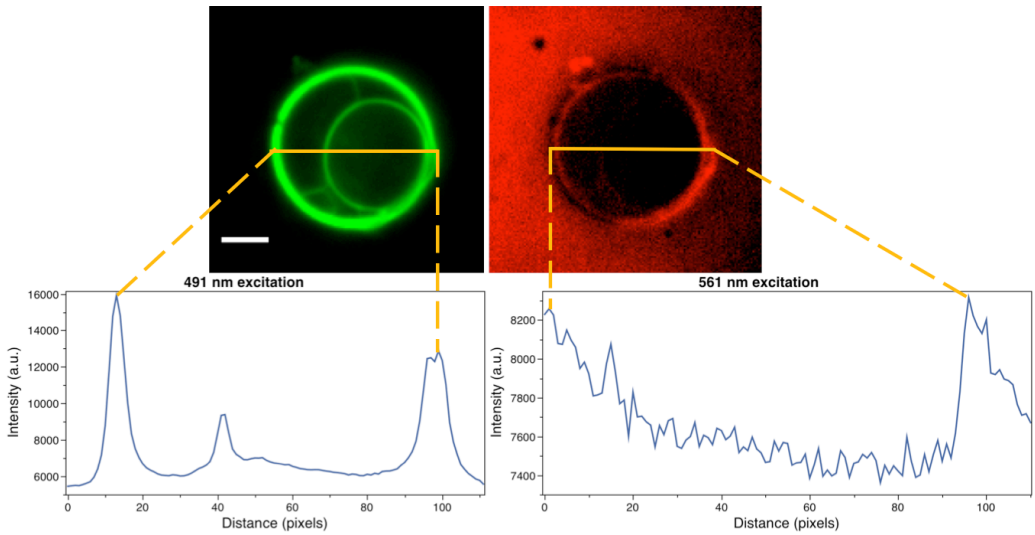

Figure S3. Confocal slice of GUVs at 491 nm (left) and 561 nm (right) excitation with corresponding intensity plots. This image shows a large GUV with smaller GUVs

encapsulated inside it. As indicated in the right micrograph, binding only occurs between the proteins on the surface of the outer GUV and the antibody. This is consistent with the expected membrane impermeability of a high-molecular-weight protein. Scale bar is 5 μm.

Identification of Liquid Ordered Phase

In order to confirm the partitioning of ATTO-488-DPPE into the liquid disordered region of phase separated vesicles the bright and dark regions of GUVs were quantified. The liquid disordered phase is primarily made up of POPC or DOPC while the liquid ordered phase is primarily cholesterol and BSM and/or DPPC. We plotted ratios of bright pixels to total GUV size (in pixels) in micrographs as a function of lipid composition (see Figure S4C). Furthermore vesicles fluorescently tagged with rhodamine-DPPE, which is known to partition into the liquid disordered phase,[5] were also fabricated and morphology of phase separated ATTO vesicles were compared.

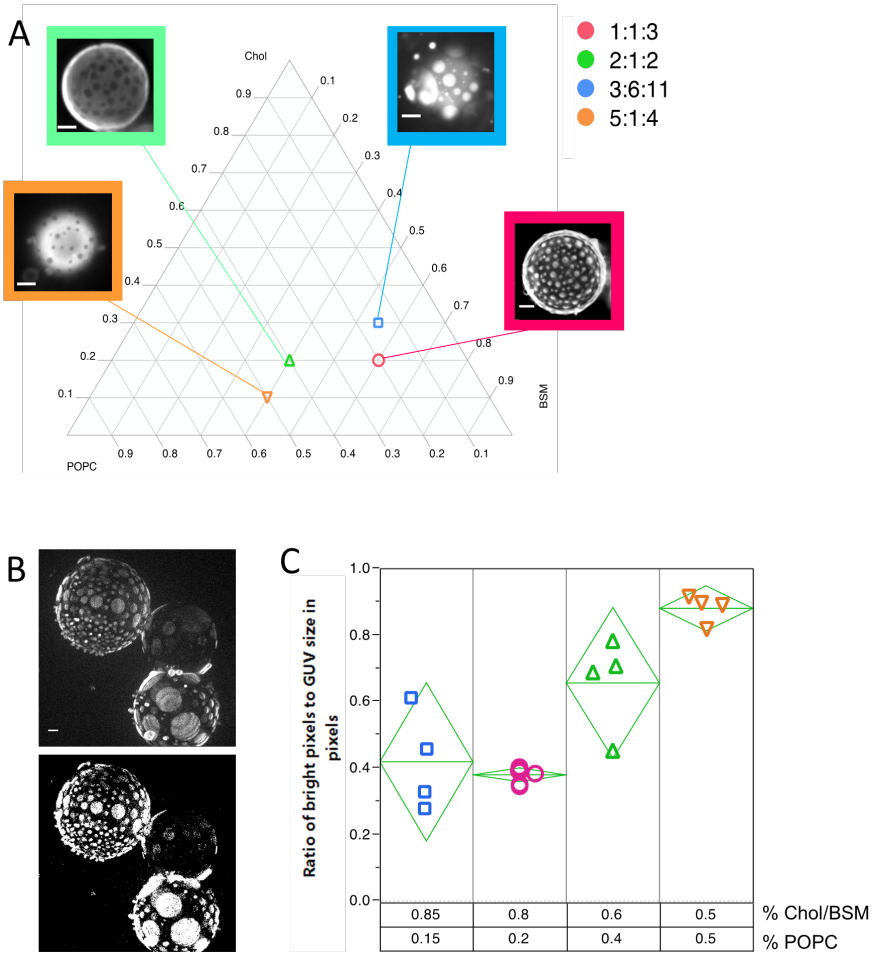

Figure S4. Quantification of sizes of bright domains identifies them as liquid disordered. A) Shows a ternary plot of POPC:Chol:BSM indicating the four compositions used in investigations with representative images of their morphologies. B) An example of a GUV micrograph of the 1:1:3 composition as taken under 491nm (top) and then made binary in ImageJ (bottom). Scale bar is 5 μm. C) Variability plot of ratio of bright pixels

to total GUV size versus concentrations of liquid ordered-preferring lipids (%Chol + %BSM) and liquid disordered-preferring lipids (%POPC).

To quantify the regions of bright and dark in phase separated vesicles, representative images were thresholded to binary and the number of white pixels was compared to the number of black pixels each GUV. 1:1:3, 2:1:2, 5:1:4, and 3:6:11 POPC:BSM:Chol compositions ($n = 4$ for each composition) were used in order to span the phase separation envelope as previously described by Veatch *et al*. (see Figure S4A).[3] Figure S4B shows an example of an image made binary and C shows a plot of the ratio of bright pixels to total GUV area versus the composition in terms of liquid ordered-preferring (cholesterol and BSM) and disordered-preferring (POPC) lipids. The plot clearly shows that as the concentration of cholesterol and BSM is decreased in the system, the ratio of bright pixels to dark pixels increases. Since this system has previously been shown to exhibit liquid/liquid phase coexistence at the temperature we studied here,[4] the bright region can be identified as a liquid disordered phase while the dark region is a liquid ordered phase.

Figure S5 shows images of phase-separated vesicles tagged with rhodamine-DPPE alongside phase separated vesicles of the same composition tagged with ATTO-488-DPPE. Rhodamine-DPPE has been previously reported to partition into the liquid disordered phase.[5] Therefore qualitative comparison of the morphologies of the vesicles makes it apparent that ATTO-488-DPPE partitions into the liquid disordered phase of vesicles. This further confirms the segregation of 5-HT_{1A} into the liquid disordered phase or bright region of phase separated GUVs.

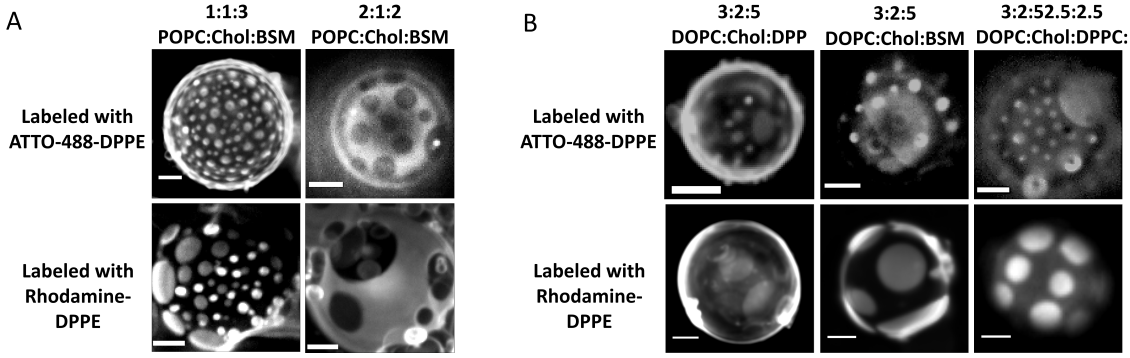

Figure S5. Qualitative comparison of phase-separated GUVs labeled with ATTO-488-DPPE (Top) and GUVs labeled with rhodamine-DPPE (Bottom). Micrographs in S5A (left) correspond to POPC:Chol:BSM lipid compositions at 1:1:3 and 2:1:2. Micrographs in S5B (right) correspond to DOPC:Chol:BSM/DPPC compositions as listed. The micrograph for POPC:Chol:BSM 2:1:2 labeled with ATTO-488-DPPE is a confocal slice. All other images are Z-stack projections. Rhodamine-DPPE has been previously reported to partition into the liquid disordered region of synthetic lipid bilayers and qualitative comparison confirms that ATTO-488-DPPE also partitions into the liquid disordered region of phase-separated GUVs.

Phase separation at varying cholesterol concentrations

Figure S6 shows phase separation in GUVs with and without 5-HT_{1A} at phase-separating compositions in which the total concentration of cholesterol in the system has been varied from 10% to 30%. In all cases, the protein continues to segregate with the liquid disordered phase.

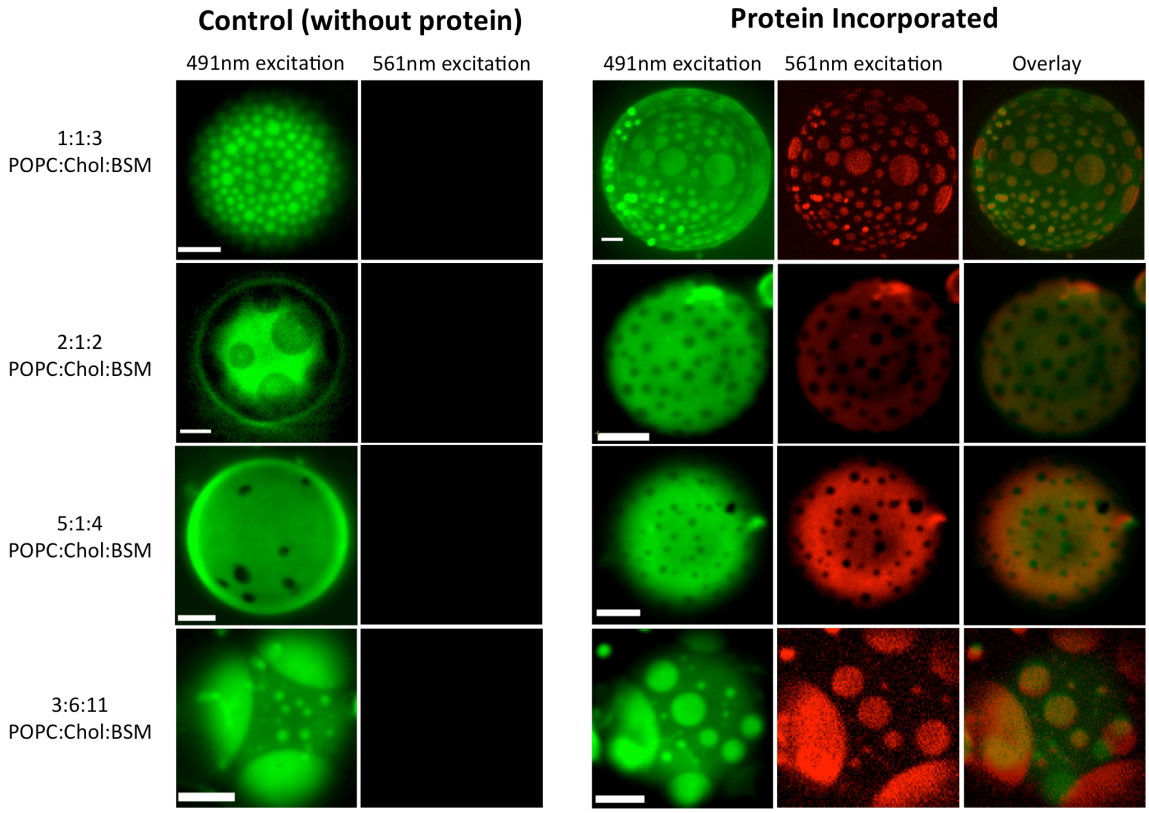

Figure S6. POPC-based vesicle compositions after antibody binding. The pairs of images on the left show controls without 5-HT_{1A}. 491 nm excitation is in the left image of each pair; 561 nm excitation is on the right. No antibody binding is apparent. The triptychs of images on the right show GUVs with 5-HT_{1A} after incubation with antibody. In each triptych, excitation at 491 nm is on the left, 561 nm is in the center, and an overlay is on the right. Overlaid images indicate the preferential segregation of 5-HT_{1A} into the liquid disordered phase (bright region) across a range of cholesterol concentrations. The image 491 nm 2:1:2 POPC:Chol:BSM protein-free control is a confocal slice, all other images are Z-projections. Scale bars are 5 μm.

Negative controls for ligand binding

Figure S7 shows examples of protein-free control vesicles that have been incubated with the fluorescent 5-HT_{1A} ligand. No association between the ligand and the GUV is apparent in the absence of protein.

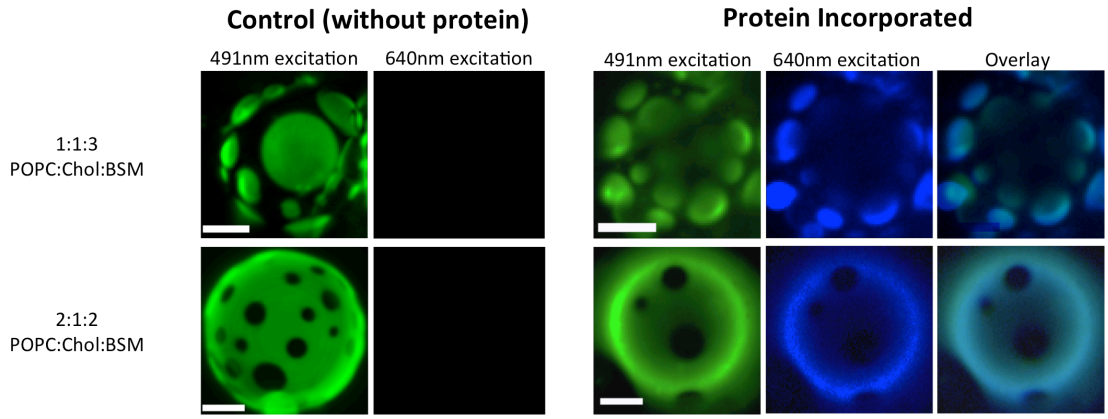

Figure S7. POPC-based GUVs after incubation with the fluorescent 5-HT_{1A} ligand. The pairs of images on the left show controls without 5-HT_{1A}. Micrographs are shown at 491 nm (left) and 640 nm (right) excitation. No ligand binding is apparent. The triptychs of images on the right show GUVs with 5-HT_{1A}. In each triptych, excitation at 491 nm is on the left, 640 nm is in the center, and an overlay is on the right. Scale bars are 5 μm.

Negative controls for antibody binding in DOPC-based systems

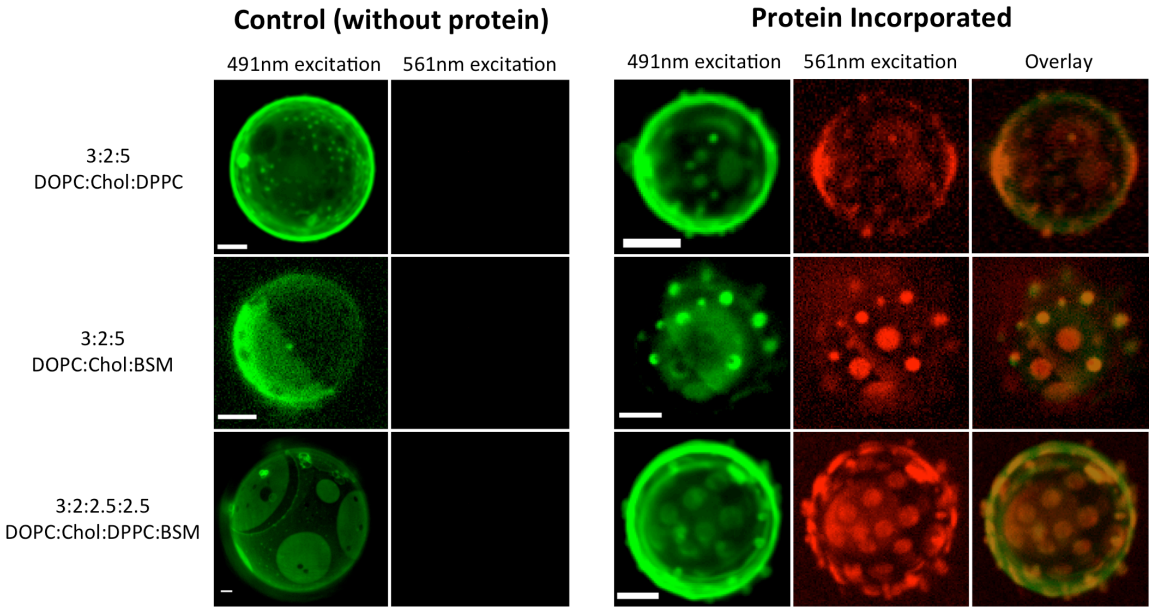

Figure S8. Confocal slices of DOPC-based GUV compositions after antibody binding. The pairs of images on the left show controls without 5-HT_{1A}. Micrographs are shown at 491 nm (left) and 561 nm (right) excitation. No apparent non-specific antibody binding occurs. The triptychs of images on the right show GUVs with 5-HT_{1A}. In each triptych, excitation at 491 nm is on the left, 561 nm is in the center, and an overlay is on the right. Scale bars are 5 μm.

References

(1) Hansen, J.; Thompson, J.; Helix-Nielsen, C.; Malmstadt, N. *J. Am. Chem. Soc.* **2013**, *135*, 17294-17297.
(2) Horger, K.; Estes, D. J.; Capone, R.; and Mayer, M. *J. Am. Chem. Soc.* **2009**, *131*, 1810-1819.
(3) Veatch, S. L.; Keller, S. L. *Phys Rev Lett* **2005**, *94*, 148101.
(4) Dietrich, C.; Bagatolli, L. A.; Volovyk, Z. N.; Thompson, N. L.; Levi, M.; Jacobson, K.; Gratton, E. *Biophys .* **2001**, *80*, 1417-1428.
(5) Baumgart, T.; Hunt, G.; Farkas, E. R.; Webb, W. W.; Feigenson, G. W. *Biochim Biophys Acta*. **2007**, *1768*, 2182-2194.